

Short communication

# Synthesis and electrochemical properties of $(\text{Pr-Nd})_{1-y}\text{Sr}_y\text{MnO}_{3-\delta}$ and $(\text{Pr}_{1-x}\text{Nd}_x)_{0.7}\text{Sr}_{0.3}\text{MnO}_{3-\delta}$ as cathode materials for IT-SOFC

Mingfei Liu, Dehua Dong, Lei Chen, Jianfeng Gao, Xingqin Liu, Guangyao Meng\*

*USTC Laboratory for Solid State Chemistry & Inorganic Membranes, Department of Materials Science and Engineering, University of Science and Technology of China (USTC), Hefei 230026, PR China*

Received 23 August 2007; received in revised form 11 October 2007; accepted 11 October 2007

Available online 18 October 2007

## Abstract

$(\text{Pr-Nd})_{1-y}\text{Sr}_y\text{MnO}_{3-\delta}$  (P-NSM,  $y=0.2, 0.25, 0.3, 0.35$ ) powders made from commercial Pr–Nd mixed oxide, as well as  $(\text{Pr}_{1-x}\text{Nd}_x)_{0.7}\text{Sr}_{0.3}\text{MnO}_{3-\delta}$  (PN3SM,  $x=0, 0.5, 0.7, 1$ ) were synthesized by a glycine-nitrate process and characterized as cathode materials for intermediate temperature solid oxide fuel cell (IT-SOFC). XRD patterns showed the powders had formed pure perovskite phase after being calcined at 800 °C for 2 h.  $(\text{Pr-Nd})_{0.7}\text{Sr}_{0.3}\text{MnO}_{3-\delta}$  (P-N3SM) achieved a high conductivity of  $194 \text{ S cm}^{-1}$  at 500 °C and showed a good chemical stability against YSZ at 1150 °C. And the thermal expansion coefficient of P-N3SM/YSZ cathode was  $11.1 \times 10^{-6} \text{ K}^{-1}$ , which well matched YSZ electrolyte film. The tubular SOFC with P-N3SM/YSZ cathode exhibited the maximum power densities of 415, 367, 327 and 282 mW  $\text{cm}^{-2}$  at 850, 800, 750 and 700 °C, respectively, which indicated P-N3SM was potentially applied in SOFC for low cost.

© 2007 Elsevier B.V. All rights reserved.

**Keywords:** Solid oxide fuel cell; Cathode; Pr–Nd mixed oxides; Tubular; Perovskite

## 1. Introduction

Solid oxide fuel cell (SOFC) is the most efficient device among the energy technology invented so far for the conversion of chemical fuels directly into electrical power [1,2]. The development of intermediate temperature SOFC (IT-SOFC) can widen the materials chosen, decrease material degradation, prolong the lifetime and reduce the cost that may accelerate the commercialization of SOFCs. However, a major issue produced by the reduced operating temperature is the decrease in the catalytic activity of the cathode for oxygen reduction [3].

The most promising cathode materials are the mixed conducting perovskite oxides. The state-of-the-art cathode material  $\text{La}_{1-x}\text{Sr}_x\text{MnO}_{3-\delta}$  (LSM) perovskite oxides are widely investigated as promising cathodes for high temperature ( $\sim 1000$  °C) operation [4,5]. However, as the temperature decreases, the cathode/electrolyte interface resistance increases rapidly due to poor oxygen-ion conductivity.

In order to improve the cathode performance, many other perovskite which exhibit high mixed oxygen-ion and electron conductivity, like  $\text{La}_x\text{Sr}_{1-x}\text{Co}_y\text{Fe}_{1-y}\text{O}_{3-\delta}$  (LSCF) [6],  $\text{Ln}_{0.6}\text{Sr}_{0.4}\text{Co}_{0.2}\text{Fe}_{0.8}\text{O}_{3-\delta}$  ( $\text{Ln}=\text{Ce, Gd, Sm, Dy}$ ) [7],  $\text{La}_x\text{Sr}_{1-x}\text{CoO}_{3-\delta}$  (LSC) [8],  $\text{Ba}_{0.5}\text{Sr}_{0.5}\text{Co}_{0.8}\text{Fe}_{0.2}\text{O}_{3-\delta}$  (BSCF) [9,10] and  $\text{Sm}_{0.5}\text{Sr}_{0.5}\text{CoO}_{3-\delta}$  (SSC) [11,12], have been applied as the cathode for IT-SOFC. However, the disadvantages, such as high thermal expansion coefficient, cobalt migration and high cost of cobalt element, restrict their application in SOFC. Hence, it is an urgent task now to develop a less expensive cathode with high performance that can be used at a relatively low temperature.

It has been reported that the LSM with either pure Pr or Nd as a substitute has higher electrochemical properties and much less reactivity with  $\text{Y}_2\text{O}_3$ -stabilized  $\text{ZrO}_2$  than LSM at intermediate temperature [13–16]. However, the performance of LSM with Pr–Nd mixture as substitutes has not been reported. As is known to all, the elements of Pr and Nd always co-exist in the minerals. It apparent that it is worthy to utilize commercial mixed Pr + Nd powder instead of pure Pr or Nd to prepare cathode materials in order to reduce the fabrication cost.

In the present study,  $(\text{Pr-Nd})_{1-y}\text{Sr}_y\text{MnO}_{3-\delta}$  (P-NSM,  $y=0.2, 0.25, 0.3, 0.35$ ) and  $(\text{Pr}_{1-x}\text{Nd}_x)_{0.7}\text{Sr}_{0.3}\text{MnO}_{3-\delta}$  (PN3SM,  $x=0,$

\* Corresponding author. Tel.: +86 551 3603234; fax: +86 551 3607627.

E-mail addresses: [mfliu@mail.ustc.edu.cn](mailto:mfliu@mail.ustc.edu.cn) (M. Liu), [mgym@ustc.edu.cn](mailto:mgym@ustc.edu.cn) (G. Meng).

0.5, 0.7, 1) (PNSM) powders were synthesized by a glycine-nitrate process and characterized as cathode materials. For the potential application in SOFCs, the chemical compatibility of P-N3SM with YSZ electrolyte was investigated, and the electrochemical properties of it were also tested in cell.

## 2. Experimental

### 2.1. Preparation of PNSM powders

Fine powders  $(\text{Pr-Nd})_{1-y}\text{Sr}_y\text{MnO}_{3-\delta}$  (P-NSM,  $y=0.2, 0.25, 0.3, 0.35$ ) and  $(\text{Pr}_{1-x}\text{Nd}_x)_{0.7}\text{Sr}_{0.3}\text{MnO}_{3-\delta}$  (PN3SM,  $x=0, 0.5, 0.7, 1$ ) were synthesized by a glycine-nitrite process [17]. Stoichiometric amount of the  $\text{Pr}_6\text{O}_{11}$ ,  $\text{Nd}_2\text{O}_3$ ,  $\text{SrCO}_3$ ,  $\text{MnCO}_3$  (all in 99.9%, Sinopharm Chemical) and Pr–Nd mixed oxides (99%, Chengdu Henry Advanced Materials Ltd., 26 mol% Pr) were dissolved in calculated amount of nitric acid. Glycine, which was used as complexation/polymerization agent, was then added with glycine/metal mole ratio set at 1.6:1. This solution was stirring on a heating plate until it changed into black foam and finally ignited to flame, forming the primary powders. The as-synthesized powders were subsequently calcined at  $800^\circ\text{C}$  for 2 h to get fine P-NSM and PN3SM powders. The phases of the fine powders were identified by X-ray diffraction (XRD) analysis on Philips PW 1730 diffractometer using  $\text{Cu K}\alpha$  radiation.

### 2.2. Measurement of electrical conductivity and thermal expansion behavior

The fine powders were ball milled in an ethanol medium for 24 h and dried subsequently. Rectangular bar specimens were then prepared by pressing the powder under 360 MPa and sintered in air at  $1350^\circ\text{C}$  for 5 h. The heating rate was fixed at  $1^\circ\text{C min}^{-1}$  below  $500^\circ\text{C}$  and  $2^\circ\text{C min}^{-1}$  between 500 and  $1350^\circ\text{C}$ . The electrical conductivity of the specimens was studied using a standard dc four-probe technique on H.P. multimeter (Model 34401) from 500 to  $800^\circ\text{C}$ .

To examine the thermo-mechanical compatibility of the materials with other component such as electrolyte, the sintered specimens were underwent thermal expansion measurement on a dilatometer, SHIMADZU50 at temperatures ranging from 20 to  $1000^\circ\text{C}$  at a heating rate of  $10^\circ\text{C min}^{-1}$ .

### 2.3. Fabrication of tubular cell with PNSM as the cathode

The cell components were selected as follows: NiO/YSZ, YSZ and P-N3SM/40 wt% YSZ (P-N3SM/YSZ) were used as anode, electrolyte and cathode materials, respectively. The tubular anode support with out diameter of 7 mm and wall thickness of 1 mm were fabricated by a extrude technique and then thin YSZ electrolyte layer was deposited on the outer surface fabricated as described in the previous study [18]. A suspension of P-N3SM/YSZ powder was prepared by mixing and ball-milling the two powders in ethanol for 24 h. Cathode layer was then prepared by spraying the suspension on the electrolyte surface [19], followed by sintering at  $1150^\circ\text{C}$  for 2 h.

### 2.4. Cell performance testing

The single tubular cell was sealed on a steel tube with silver paste, and electrochemically tested in a self-assembled cell testing system with humidified hydrogen (3%  $\text{H}_2\text{O}$ ) as fuel and stationary air as oxidant. The cell voltage and output current of the cells were measured with digital multimeters (CDM-8145). The polarization resistances of the cell were measured using a two-probe impedance spectroscopy (Chi604a, Shanghai, Chenhua) under open circuit voltage (OCV) mode with amplitude of 5 mV over the frequency range of 0.01 Hz to 100 kHz. A scanning electron microscope was used to observe the microstructure of the cells after testing.

## 3. Results and discussion

XRD patterns of fine PNSM powder samples with various compositions are shown in Fig. 1. It can be seen that the major peaks are well indexed and almost the same as  $\text{Nd}_{0.7}\text{Sr}_{0.3}\text{MnO}_3$  (JCPDS card no. 86-1534), showing the single orthorhombic perovskite-type structure. And the very small peaks occurred for the compositions with mixed Pr and Nd oxides, may come from the impurity in the mixed Pr and Nd oxide source, the influence of which on the cathode property needs to examine.

Fig. 2(a and b) shows the temperature dependence of the electrical conductivity of the samples on compositions. A good linearity between  $\log(\sigma T)$  and the reciprocal absolute temperature is found over a wide temperature range from 500 to  $800^\circ\text{C}$ , indicating that the conduction may be explained by the small polaron hopping mechanism[16,20]:

$$\sigma = \frac{A}{T} \exp\left(-\frac{E_a}{RT}\right) \quad (1)$$

where  $\sigma$  is electrical conductivity,  $A$  is a constant,  $R$  is gas constant and  $E_a$  is the activation energy of conduction. For P-NSM, electrical conductivity significantly increased with the increase of the Sr substitution and a sample with Sr substitution of 0.3 reached a maximum value of  $216 \text{ S cm}^{-1}$  at  $800^\circ\text{C}$ , which is

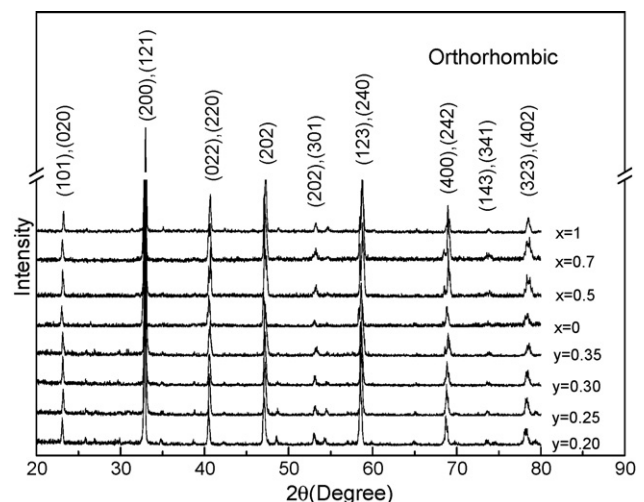


Fig. 1. XRD patterns of various compositions of fine PNSM powders.

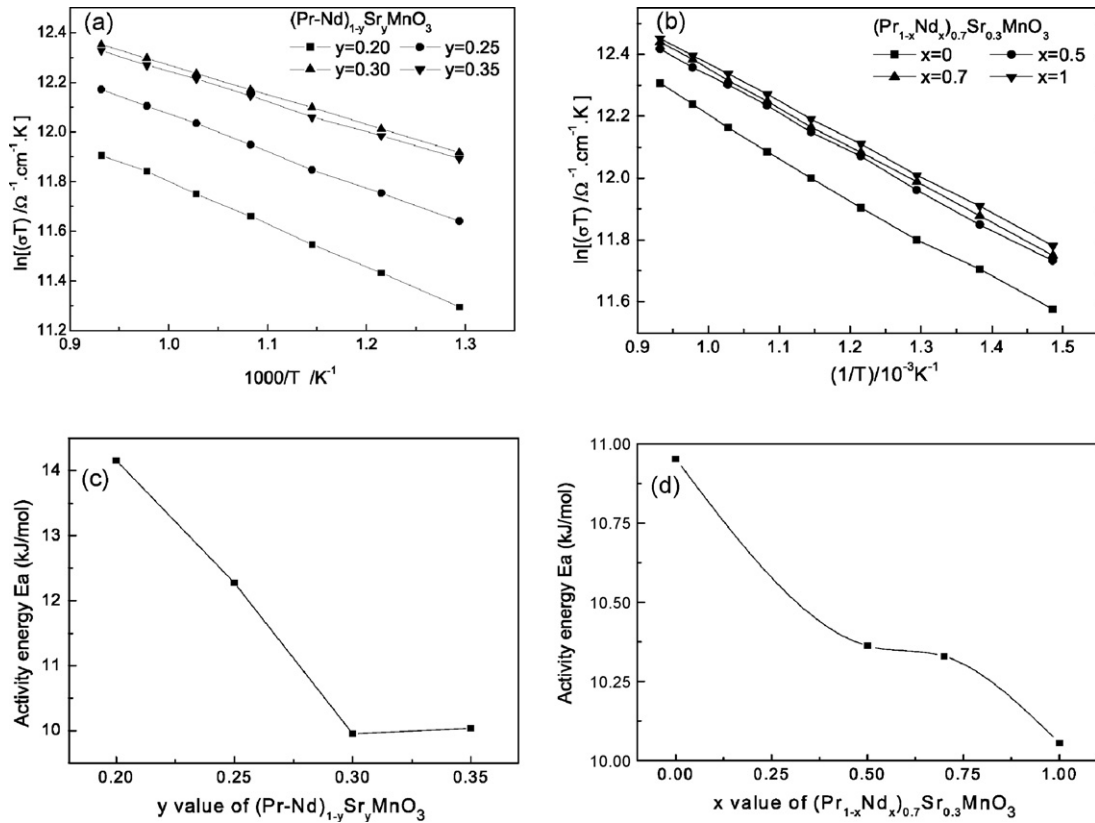


Fig. 2. Electrical conductivity and activity energy of PNSM with various compositions. (a) The electrical conductivity of P-N3SM with difference Sr content; (b) the activity energy of PN3SM with difference Nd content; (c) the electrical conductivity of P-N3SM with difference Sr content; (d) the activity energy of PN3SM with difference Nd content.

higher than LSM [21]. The values of  $E_a$  calculated from the plots of Fig. 2(a) by linear regression are given in Fig. 2(c). As can be seen, activity energy decreased from 14.1 to 9.9  $\text{kJ mol}^{-1}$ . With further increasing of the Sr substitution to 0.35, the conductivity had little change. The effect on Pr–Nd content in terms of the electrical conductivities is shown in Fig. 2(b). The electrical conductivity increased as the amount of Nd content increased, and achieved 206, 230, 235 and 238  $\text{S cm}^{-1}$  at 800 °C as  $x = 0, 0.5, 0.7$  and 1, respectively. The activity energies of the specimens are all about 10–11  $\text{kJ mol}^{-1}$ , which suggested that the amount of Nd had little effect on the conductivity of the materials. The values of electrical conductivities and activity energies of pure Nd doped LSM in our work were similar to the values reported by Kostoglou and Ftikos [16]. The little difference between P-N3SM and PN3SM may be due to different purity of the primary materials used in the preparation. Therefore, the P-N3SM would be a good choice for SOFC materials. In order to improve cathode adhesion and extend cathode active zone, the electrolyte powders are always added as a part of cathode. Hence, the subsequent researches are based on P-N3SM/YSZ as composite cathode material for SOFC.

In order to simulate the SOFC cathode preparation and operating condition, some tests are made on the XRD and thermal expansion behavior of P-N3SM/YSZ pellet after sintering at 1150 °C for 2 h in the air. The XRD pattern of P-N3SM/YSZ pellet is shown in Fig. 3. It can be found that P-N3SM does not react with YSZ as the diffraction patterns clearly depict two

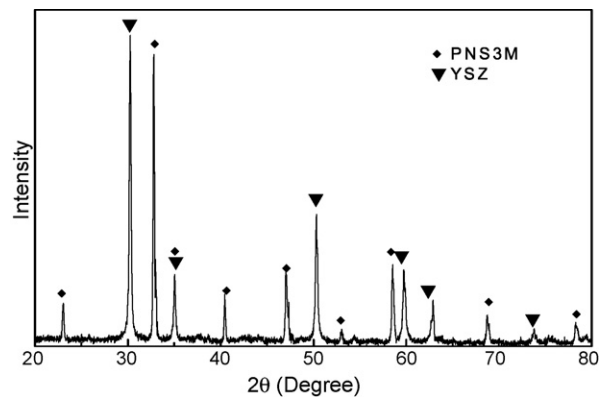


Fig. 3. XRD pattern of the mixture of YSZ and P-N3SM after sintering at 1150 °C for 2 h.

groups of diffraction peaks. One group belongs to the P-N3SM and the other is cubic phase of  $\text{ZrO}_2$ . So the X-ray diffraction results indicate that P-N3SM is chemically stable against YSZ at operating temperature.

The TEC value of P-N3SM/YSZ is  $11.1 \times 10^{-6} \text{K}^{-1}$  between 350 and 1000 °C, which is very close to that of YSZ electrolyte,  $10.8 \times 10^{-6} \text{K}^{-1}$ . The small mismatch in TEC between P-N3SM/YSZ and YSZ can be beneficial for the SOFC system in maintaining long-term stability and enduring thermal cycle.

The cross-sectional fracture of the tubular anode-supported cell with P-N3SM/YSZ cathode was shown in Fig. 4. The

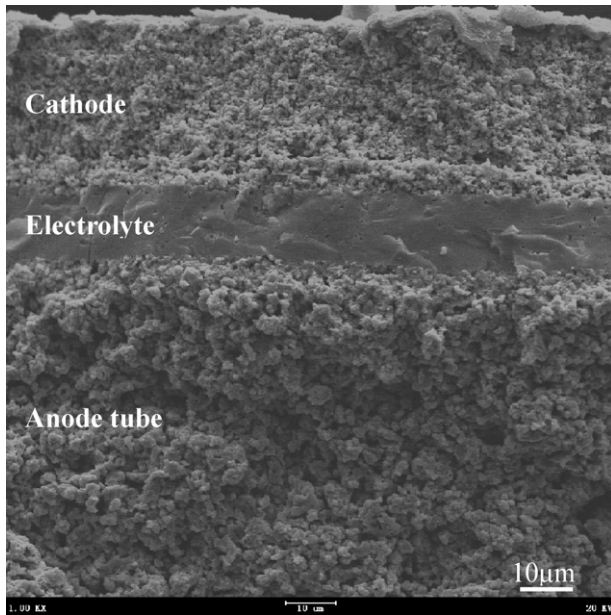


Fig. 4. Cross-sectional fractured surface micrograph of the cell after testing.

cathode has a homogeneous porous structure and is coherent very well to YSZ membrane, and the thickness of the electrolyte and cathode is about 15 and 30  $\mu\text{m}$ , respectively. The P-N3SM with 40 wt%SDC is also used to prepare the cathode film on YSZ membrane using the same method, but it cannot get a good adhesion with YSZ membrane. So the addition of YSZ in cathode could improve the cathode/electrolyte interface, which can be seen from Fig. 4.

The current–voltage ( $I$ – $V$ ) and current–power ( $I$ – $P$ ) curves of the cell tested at 700–850  $^{\circ}\text{C}$  is shown in Fig. 5. As can be seen from the curves, the maximum power densities of 415, 367, 327 and 282  $\text{mW cm}^{-2}$  with the OCV of 1.04, 1.06, 1.07 and 1.08 V are achieved at 850, 800, 750 and 700  $^{\circ}\text{C}$ , respectively. Although the performance characteristics of the tubular cell with P-N3SM/YSZ cathode is still not as high as we hoped and still lower than that of planar SOFC, the performance achieved in the tubular SOFC is encouraging. In order to further improve the performance of the tubular cell, a simple calculation based on electricity was used

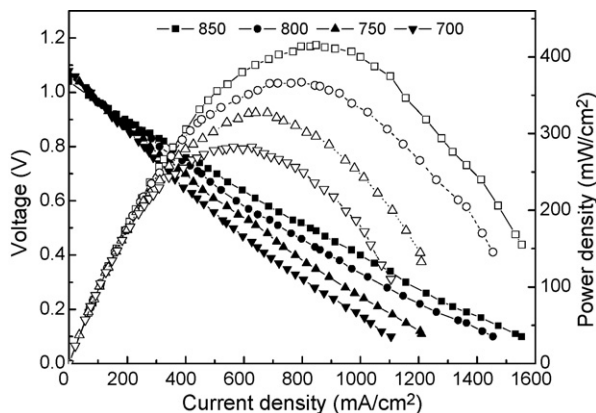


Fig. 5. The  $I$ – $V$  and  $I$ – $P$  curves of the tubular cell with P-N3SM/YSZ cathode.

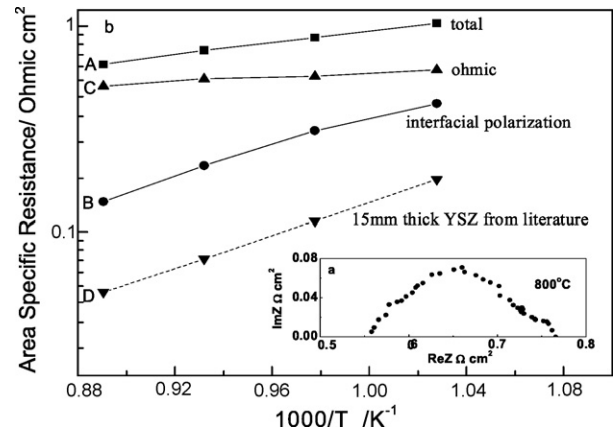


Fig. 6. (a) Impedance spectra of a single cell as measured at 800  $^{\circ}\text{C}$  and (b) the ASR of the total cell resistances, total ohmic resistance, interfacial polarization resistances and electrolyte resistance (estimated from literature) at different temperature.

for investigating the factor that influenced the cell performance.

We assume that the total areal specific resistance of a cell (i.e.  $R_{\text{internal}}$ ) is constant as a function of current density, when the power is output from a cell, the maximum power can be calculated by Eq. (2):

$$P_{\text{max}} = \frac{V_{\text{OCV}}^2}{4R_{\text{internal}}} \quad (2)$$

where  $V_{\text{OCV}}$  is the open circuit voltage,  $R_{\text{internal}}$  is the total areal specific resistance of the cell,  $P_{\text{max}}$  is the maximum power density. So we can use Eq. (2) to estimate the total resistance of the cell, which is shown in the curve A in Fig. 6.

For a single cell, the total internal resistances mainly come from two parts:

- (1) The area specific polarization resistances of the two interfaces: the cathode–electrolyte interface and the anode–electrolyte interface. The total interfacial polarization resistances were determined from the impedance spectra, the values were 0.14, 0.21, 0.31 and 0.42  $\Omega \text{ cm}^2$  at 850, 800, 750 and 700  $^{\circ}\text{C}$ , respectively, which was shown in Fig. 6 curve B.
- (2) The ohmic resistance, including the cathode, anode, electrolyte and wire, etc., was shown in Fig. 6 curve C. Compared with the electrolyte, the cathode and anode resistance can be ignored. The electrolyte resistance can be estimated by Eq. (3):

$$r = \frac{l}{\sigma} \quad (3)$$

where  $r$  is the areal specific ohmic resistance;  $\sigma$  is the conductivity;  $l$  is the thickness of the electrolyte. The electrolyte resistance of 15  $\mu\text{m}$  thick with an area of 1  $\text{cm}^2$  can be estimated to be about 0.051, 0.074, 0.113 and 0.180  $\Omega \text{ cm}^2$  at 850, 800, 750 and 700  $^{\circ}\text{C}$  (the conductivity is from literature data [22]), respectively. The resistance of electrolyte was shown in Fig. 6 curve D. Taking



the existence of some closed pores into account, the resistance may be a little higher than the value of calculation.

It can be seen from Fig. 6 that the ASR of the ohmic part appeared to be about 0.43–0.48  $\Omega \text{ cm}^2$  higher than the estimated value of YSZ film, which might result from the method of current collection as the resistance of wire was very small (Ag wire was used to collect the current). Therefore, if the method of current collection ameliorated, the cell performance could be highly improved.

#### 4. Conclusions

The P-N3SM and PN3SM powders were synthesized by a glycine-nitrate process to be used as cathode materials for SOFC. The electrical conductivity of P-N3SM made from Pr–Nd mixed oxide was 215  $\text{S cm}^{-1}$  at 800 °C, which could be compared with that of PN3SM made from high pure  $\text{Pr}_6\text{O}_{11}$  and  $\text{Nd}_2\text{O}_3$  powders. The average thermal expansion coefficient of P-N3SM/YSZ was  $11.1 \times 10^{-6} \text{ K}^{-1}$ , which was very close to that of YSZ electrolyte film. A single tubular cell with the composite cathode achieved the power densities of 415, 367, 327 and 282  $\text{mW cm}^{-2}$  at 850, 800, 750 and 700 °C, respectively. The results suggested that the P-N3SM was a good choice of cathode materials for IT-SOFC with low cost.

#### Acknowledgement

The authors gratefully acknowledge the support of this research by National Natural Science Foundation of China under contract No. 50572099.

#### References

- [1] N.Q. Minh, *J. Am. Ceram. Soc.* 76 (1993) 563.
- [2] H.C. Yu, F. Zhao, A.V. Virkar, K.Z. Fung, *J. Power Sources* 152 (2005) 22.
- [3] M.T. Colomer, B.C.H. Steele, J.A. Kilner, *Solid State Ionics*, 147 (2002) 41.
- [4] T. Horita, K. Yamaji, M. Ishikawa, N. Sakai, H. Yokokawa, T. Kawada, T. Kato, *J. Electrochem. Soc.* 145 (1998) 3196.
- [5] J. Mizusaki, Y. Yonemura, H. Kamata, K. Ohyama, N. Mori, H. Takai, H. Tagawa, M. Dokiya, K. Naraya, T. Sasamoto, H. Inaba, T. Hashimoto, *Solid State Ionics* 132 (2000) 167.
- [6] E.P. Murray, M.J. Sever, S.A. Barnett, *Solid State Ionics* 148 (2002) 27.
- [7] J.F. Gao, X.Q. Liu, D.K. Peng, G.Y. Meng, *Catal. Today* 82 (2003) 207.
- [8] V.V. Srdić, R.P. Omorjan, J. Seydel, *Mater. Sci. Eng. B* 116 (2005) 119.
- [9] B. Wei, Z. Lü, X.Q. Huang, S.Y. Li, G. Ai, Z.G. Liu, We.H. Su, *Mater. Lett.* 60 (2006) 3642.
- [10] Z.P. Shao, S.M. Haile, *Nature* 431 (2004) 170.
- [11] C.R. Xia, W. Rauch, F.L. Chen, M.L. Liu, *Solid State Ionics* 149 (2002) 11.
- [12] N.P. Bansal, Z.M. Zhong, *J. Power Sources* 158 (2006) 148.
- [13] T. Ishihara, T. Kudo, H. Matsuda, Y. Takita, *J. Electrochem. Soc.* 142 (1995) 1519.
- [14] S.T. Aruna, M. Muthuraman, K.C. Patil, *Solid State Ionics* 120 (1999) 275.
- [15] T.L. Wen, H. Tu, Z. Xu, O. Yamamoto, *Solid State Ionics* 121 (1999) 25.
- [16] G.Ch. Kostogloudis, Ch. Ftikos, *J. Eur. Ceram. Soc.* 19 (1999) 497.
- [17] L.A. Chick, L.R. Pederson, G.D. Maupin, *Mater. Lett.* 10 (1990) 6.
- [18] D. Dong, M. Liu, Y. Dong, B. Lin, J. Yang, G. Meng, *J. Power Sources* 171 (2007) 495.
- [19] R.Q. Yan, D. Ding, B. Lin, M.F. Liu, G.Y. Meng, X.Q. Liu, *J. Power Sources* 164 (2007) 567.
- [20] D.P. Karim, A.T. Aldred, *Phys. Rev., B* 20 (1979) 2255.
- [21] H. Ullmann, N. Trofimenko, F. Tietz, D. Stöver, A. Ahmad-Khanlou, *Solid State Ionics* 138 (2000) 79.
- [22] K.C. Wincewicz, J.S. Cooper, *J. Power Sources* 140 (2005) 280.